공학석사 학위논문

알칼리 산업부산물을 이용하여 해수로부터 고순도 황산마그네슘 및 탄산마그네슘을 생산하는 방법

Recovery of magnesium from seawater with high purity of magnesium sulfate and magnesium carbonate using alkali industrial by-products

지도교수 김 명 진

공동지도교수 김 동 선

2020년 2월

한국해양대학교 해양과학기술전문대학원

해양과학기술융합학과

나 혜 림

본 논문을 나혜림의 공학석사 학위논문으로 인준함

위원장 : 장 재 수 인

위 원 : 김 명 진 인

위 원 : 김 동 선 인

2019년 12월

한국해양대학교 해양과학기술전문대학원

Contents

List of Tables

List of Figures

알칼리 산업부산물을 이용하여 해수로부터 고순도 황산마그네슘 및 탄산마그네슘을 생산하는 방법

나혜림

한국해양대학교 해양과학기술전문대학원
해양과학기술융합학과

초록

본 연구에서는 해수의 마그네슘을 고순도 황산마그네슘과 탄산마그네슘으로 회수하는 각 공정을 개발하였다. 각 공정은 침전, 농축, 석출의 연속된 세 단계로 구성된다. 황산마그네슘의 경우, 해수담수화농축수로부터 제조한 황산마그네슘 농축액에 에탄올을 투여해 황산마그네슘 고체를 얻는 기존 방법을, 에탄올을 두 단계로 나누어 투입하는 것으로 개선하였다. 마그네슘 농축액에 에탄올을 소량 투여하여 칼슘 불순물을 황산칼슘으로 침전시켜 제거하였고, 에탄올을 추가로 투여해 고순도 황산마그네슘을 생성하였다. 탄산마그네슘의 경우, 해수로부터 침전시킨 수산화마그네슘 슬러리에 이산화탄소를 주입하여 칼슘불순물을 쉽게 탄산칼슘 형태로 제거하였다. 탄산화 반응의 조건 중 수산화마그네슘의 농도와 이산화탄소 유량은 마그네슘 용출 효율을 향상시키는데 주요한 인자였다. 마그네슘 용출액을 방치하여 순도 높은 탄산마그네슘을 제조하였다.

Keywords: Seawater 해수; Seawater desalination brine 해수담수화농축수; Magnesium sulfate 황산마그네슘; Magnesium carbonate 탄산마그네슘; alkali industrial by-product 알칼리 산업부산물; high purity 고순도

Capture 1. Production of magnesium sulfate from seawater desalination brine

1.1. Introduction

Seawater desalination is a straightforward technique for pure water production, but it also results in brine with higher salinity and temperature than seawater. Almost 41 % of the total volume of seawater desalination brine is discharged into the sea without undergoing treatment processes (Ahmad & Baddour, 2014), which may cause hazardous environmental problems (Missimer & Maliva, 2018).

To solve these problems, many studies have been conducted on the management of brine through safe disposal or reuse of brine (Giwa, et al., 2017). The recovery of minerals from seawater desalination brine has been widely studied because it is an environmentally friendly and economic method that reduces the discharge of brine and produces valuable resources (Jeppesen, et al., 2009). Many resources that are dissolved in seawater desalination brine have been the targets of extraction, such as Mg (Casas, et al., 2014; Sorour, et al., 2014; Dong, H. et al., 2018), Li (Park, et al., 2014), Ca (Choi, Y., 2018), K (Mohammadesmaeili, et al., 2010), and Cl (Melián-Martel, et al., 2011). An evaluation of the profitability of each element recovered from seawater desalination brine via its concentration and market price implies that Mg is worth extracting from seawater desalination brine because of economic aspects, which highly depend on the purity of the final Mg product (Fig. 1) (Shahmansouri, et al., 2015).

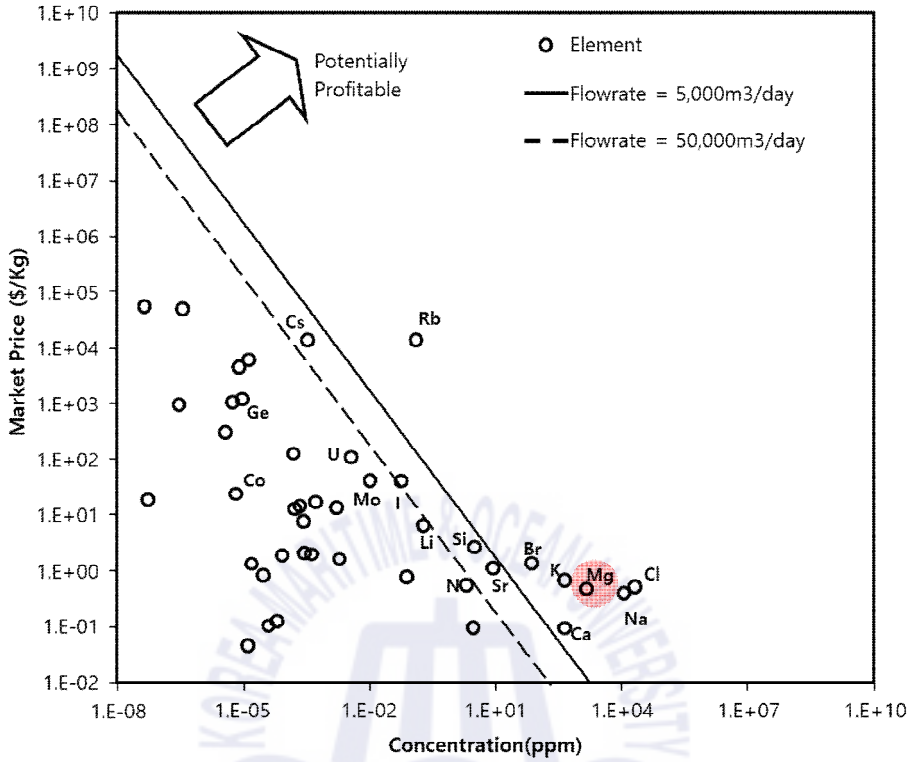

Fig. 1. Log-log plot showing concentration and market price of each mineral in the seawater desalination brine (Shahmansouri, et al., 2015).

Many novel methods for recovering Mg from seawater desalination brine have been presented, including membrane separation (Zahedi. et al., 2017), ion exchange (Pérez-González. et al.,), biocrystallization (Casas, et al., 2014), and chemical processes (Dong, et al., 2018). Zahedi et al. (Zahedi & Ghasemi, 2017) recovered 97 % of the Mg contained in seawater desalination brine using a bulk liquid membrane in 2.5 h. Pérez-González et al. used an ion-exchange resin to extract Mg from seawater desalination brine along with Ca. Wan et al. performed biomineralization experiments that precipitated the Mg of the brine in the form of a granular microstructure over 16 d.

However, currently commercialized methods for recovering Mg from brine or seawater are simple chemical precipitation methods that use lime or dolomite (Shahmansouri. et al., 2015). Alkali precipitants, such as sodium hydroxide (NaOH), ammonium hydroxide (NH_4OH), or sodium carbonate (Na_2CO_3), have been used in many studies (Dong. et al., 2018). The form of recovered Mg salts depends on the components of the precipitant, and its purity is determined either by the amount of impurities derived from the brine (such as Ca or B) or precipitant. Casas et al. obtained magnesium hydroxide ($Mg(OH)_2$) by using NaOH as a precipitant, which has a purity of approximately 52-57 % and contains approximately 3-26 % calcium carbonate ($CaCO_3$) along with a small amount of K and B. Sorour et al. recovered Mg in the form of magnesium carbonates and magnesium phosphates using Na_2CO_3 and $Na_3PO_4 \cdot 12H_2O$ as Mg precipitants in seawater desalination brine, but large amounts of Ca was also precipitated in the process. Dong et al. added NH_4OH to brine for precipitating $Mg(OH)_2$ with a purity of approximately 75.6-98 %. $CaCO_3$ was the major impurity detected, which comprised approximately 2-24.4 % of the Mg precipitate. Lehmann et al. used calcium oxide (CaO) as a Mg precipitant. In order to improve the precipitation efficiency of $Mg(OH)_2$, micro magnesite particles were added to a $Mg(OH)_2$ slurry and subsequently dissolved in acid (sulfuric acid (H_2SO_4), hydrochloric acid (HCl), and carbonic acid (H_2CO_3)). The purity of the Mg solution obtained was greater than 97 %, and the impurities contained trace amounts of B and Fe.

Instead of the expensive alkali precipitants, such as NaOH and NH_4OH, used in previous studies, we used paper sludge ash as an alkali industrial by-product. In addition, we eliminated the impurities, such as B or Ca, to

increase the purity of the final Mg product. In this study, we conducted a continuous three-step process for recovering Mg from seawater desalination brine: pre-precipitation of Mg using alkaline industrial by-products, dissolution of Mg using H_2SO_4, and precipitation of $MgSO_4$ using ethanol. The aim of this study was to derive optimal conditions not only to maximize the recovery efficiency of Mg from the brine, but also to minimize the content of impurities.

1.2 Materials and Methods

1.2.1 Materials and Analysis

The seawater desalination brine was taken from the 'A' desalination plant in Busan, South Korea and stored in a refrigerator. Paper sludge ash (PSA), which is an alkali industrial by-product, was used as the Mg precipitant and supplied by a paper mill in South Korea. We used H_2SO_4 (95 %) and ethanol (99 %) from Junsei Company. X-ray diffraction (XRD, Shimadzu, Optima 8300), X-ray fluorescence (XRF, Shimadzu, XRF-1700), and scanning electron microscopy (SEM, Tescan, MIRA-3) were used to determine the constituents and contents of the solids and the crystal form of $MgSO_4$. A laser scattering particle size analyzer (Sympatec, HELOS) was used to measure the size of the PSA. Inductively coupled plasma-optical emission spectrometry (Perkin Elmer, Optima 8300) was used to determine the concentrations of Mg, Ca, Al, Fe, Si, and B, and the pH was measured using a pH meter (Thermo, Orion Star 211)

1.2.2 Methods

1.2.1.1 Overall process overview: three-step process

The process of recovering Mg from the seawater desalination brine in the form of $MgSO_4$ was conducted in three successive steps (Fig. 2). The first step was pre-precipitation of Mg, in which a mixture of PSA and brine was prepared to precipitate the Mg ion of the brine into $Mg(OH)_2$. The second step was dissolution of Mg, wherein a mixture of PSA and $Mg(OH)_2$ was added to H_2SO_4 in order to elute Mg. The third step was precipitation of $MgSO_4$, in which ethanol was added to the eluent to precipitate $MgSO_4$. Notably, the last step could be consists of two steps to improve the purity of $MgSO_4$. In this study, the following experiments were conducted to derive the optimum conditions at each step.

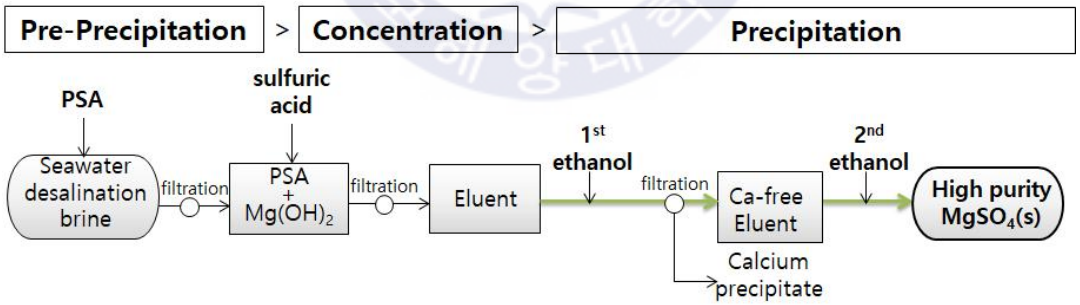

Fig. 2. Three-step process for recovering Mg from seawater desalination brine.

1.2.2.2 Pre-precipitation of Mg using PSA

We used the PSA to precipitate the Mg of the seawater desalination brine. A certain amount of PSA was mixed with 100 mL of brine and then stirred at 250 rpm for 1 h. The solid to liquid ratio of PSA and brine was controlled at ratios of 1:25 and 1:100. After filtering the suspension through a 0.45 μm membrane, the concentrations of Mg, Ca, and B and the pH of the filtrate were measured. By varying the ratios of PSA to brine, we determined the minimum amount of PSA needed to precipitate all the Mg of the brine as the optimum condition.

1.2.2.3 Dissolution of $Mg(OH)_2$ using sulfuric acid

We mixed 2.5 g of PSA with 100 mL of brine based on the optimum conditions derived from Section 3.1., and the solid was collected after the precipitation of the mixture. We prepared eight solid samples using the same method. Each solid sample was added to 20 mL of H_2SO_4 and sufficiently stirred at 250 rpm for 1 h. Here, the concentration of H_2SO_4 was varied from 0.3 M to 4.0 M. After filtering the suspension through a 0.45 μm membrane, we measured the pH and the concentrations of Mg, Ca, Al, Si, Fe, and B in the filtrate. The components of the solids were also analyzed. We determined the optimum condition of H_2SO_4 as the minimum concentration needed to dissolve the Mg as much as possible.

1.2.2.4 Precipitation of $MgSO_4$ using ethanol

1.2.2.4.1 One-step process

We prepared 6 solid samples, which were obtained by mixing 2.5 g of PSA and 100 mL of brine and filtering the mixture. The solid samples were mixed with 20 mL of 1.0 M H_2SO_4 and each mixture was stirred at 250 rpm for 1 h and then filtered through a 0.45 μm membrane to obtain the filtrate, which had a volume of about 20 mL and was called eluent. We injected ethanol into each eluent by controlling the amount of ethanol in the range of approximately 4-40 mL, which corresponded to the volume ratio of eluent to ethanol of approximately 1:0.2-1:2.0. The mixture of the eluent and ethanol stood for at least 6 h at room temperature, the solid was filtered, and the pH and the concentrations of Mg and Ca of the filtrate were measured. The solids obtained when the volume ratio of the eluent to ethanol was 1:1 were analyzed using XRD, XRF, and SEM.

1.2.2.4.2 Two-step process

1.2.2.4.2.1 Eliminating Ca impurity from Mg eluent

From '1.2.2.4.1 One-step process' when the volume ratio of eluent to ethanol is 1:0.4, we analyzed the solid and filtrate using XRD and AA, respectively.

1.2.2.4.2.2 Precipitation Mg from Ca-free Mg eluent

In the same way as '1.2.2.3 Dissolution of $Mg(OH)_2$ using sulfuric acid', we prepared 6 eluent samples. At each eluent samples 8 mL of ethanol was added and the mixture was filtrated after 6 h left at room temperature. Each of the filtrate was gained and we added the additional ethanol to filtrate varifing the amount of ethanol 4-16 mL, which is corresponding the volume ratio of eluent to total added ethanol would be 1:0.6-1:2:0. The mixture of the eluent and ethanol stood for at least 6 h at room temperature, the solid was filtered, and the pH and the concentrations of Mg and Ca of the filtrate were measured. The solids obtained when the volume ratio of the eluent to ethanol was 1:1 were analyzed using XRD, XRF, and SEM.

1.2.2.4.3 Comparing the phase purity depending on ethanol adding method

Through two different method, one-step process and two-step process, the solids obtained when the volume ratio of the eluent to ethanol was 1:1 were analyzed using XRD, XRF, and SEM.

1.3 Results and Discussion

1.3.1 Materials analysis

Table 1 shows the results of the analysis of the brine. The concentrations of Mg and Ca were 2,340 mg/L and 664 mg/L, respectively, and the pH was 7.8.

Table 1. Concentrations of Mg, Ca, and B in the seawater desalination brine used in this study.

Components	Mg	Ca	B
Concentration (mg/L)	2,340	664	6.6

Table 2. shows the components of the PSA measured using XRF. The main components of the PSA were 67 % Ca and some Si, Al, Mg, and Fe. The average particle size of the PSA was 24.5 μm (Fig. 3).

Table 2. X-ray fluorescence analyses of the paper sludge ash

Component	CaO	SiO_2	Al_2O_3	MgO	Fe_2O_3	SO_3	P_2O_5
Content (%)	67.21	15.02	6.62	4.37	1.77	2.72	0.53

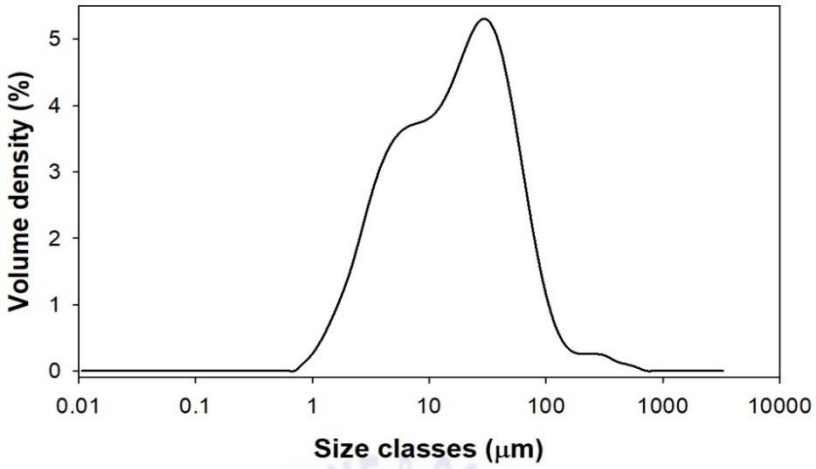

Fig. 3. Particle size distribution of PSA.

1.3.2. Pre-precipitating of Mg using PSA

Figure 4 shows the concentrations of Mg, Ca, and B and the pH of the filtrate depending on the solid to liquid ratio of PSA and brine. As the ratio of PSA to brine increased, the pH and the concentration of Ca gradually increased while the concentration of Mg decreased. When the ratio was 1:40, the concentration of Mg was 46 mg/L, which was close to zero compared with the initial Mg concentration of 2,340 mg/L, and the pH was 10.8. This was because the Mg ion in the brine precipitated in the form of $Mg(OH)_2$ (Dong. et al., 2018). Therefore, we decided that the optimum ratio of PSA to brine required for precipitating the Mg of the brine was PSA:brine = 1:40 (g:mL), and the Mg precipitation efficiency was 98 %.

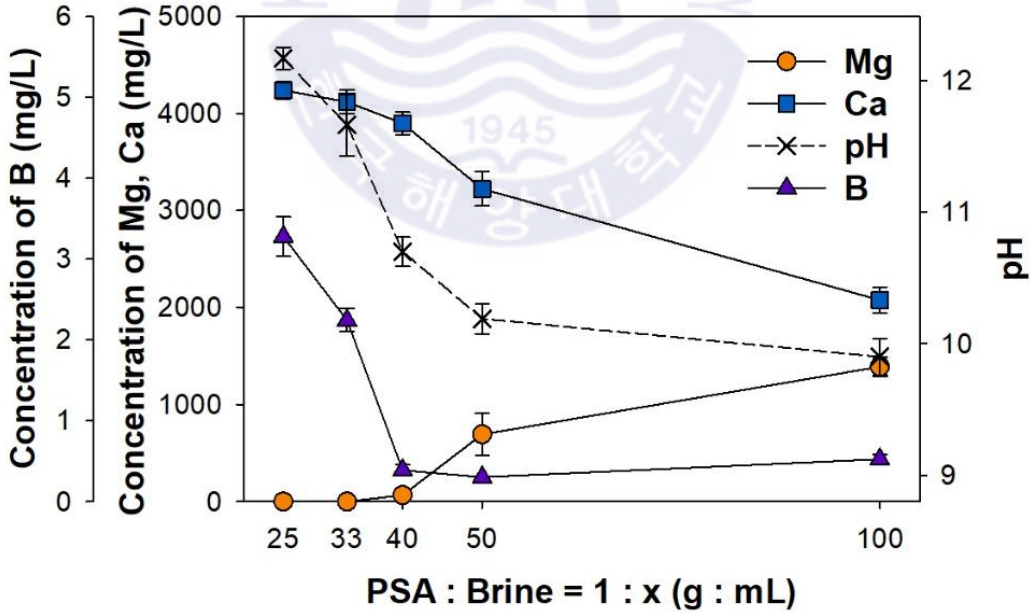

Fig. 4. Concentrations of Mg, Ca, and B and the pH of the filtrate depending on the ratio of paper sludge ash (PSA) to brine.

Figure 5(a) and 5(b) show the XRD results of the raw PSA and the solid obtained after filtering the mixture of PSA and brine when the ratio was 1:40, respectively. In Fig. 5(a), peaks of calcium hydroxide ($Ca(OH)_2$), CaO, and $CaCO_3$ were mainly observed, whereas in Fig. 5(b), only $CaCO_3$ remained. By the reaction of PSA and brine, the CaO of the PSA was hydrated to $Ca(OH)_2$, which dissolved easily in the form of Ca^{2+} and OH^-. This OH^- reacted with the Mg^{2+} of the brine to precipitate $Mg(OH)_2$. These mechanisms have already been widely used in common Mg precipitation methods (Lehmann et al., 2014; Dave and Ghosh, 2005).

$$CaO + H_2O \rightarrow Ca(OH)_2$$

$$Ca(OH)_2 \rightarrow Ca^{2+} + 2OH^-$$

$$Mg^{2+} + 2OH^- \rightarrow Mg(OH)_2$$

It was difficult to find the peaks of $Mg(OH)_2$ in Fig. 5(b) owing to the poor crystallization characteristics of $Mg(OH)_2$ (Smith et al., 2001; Barba et al., 1980).

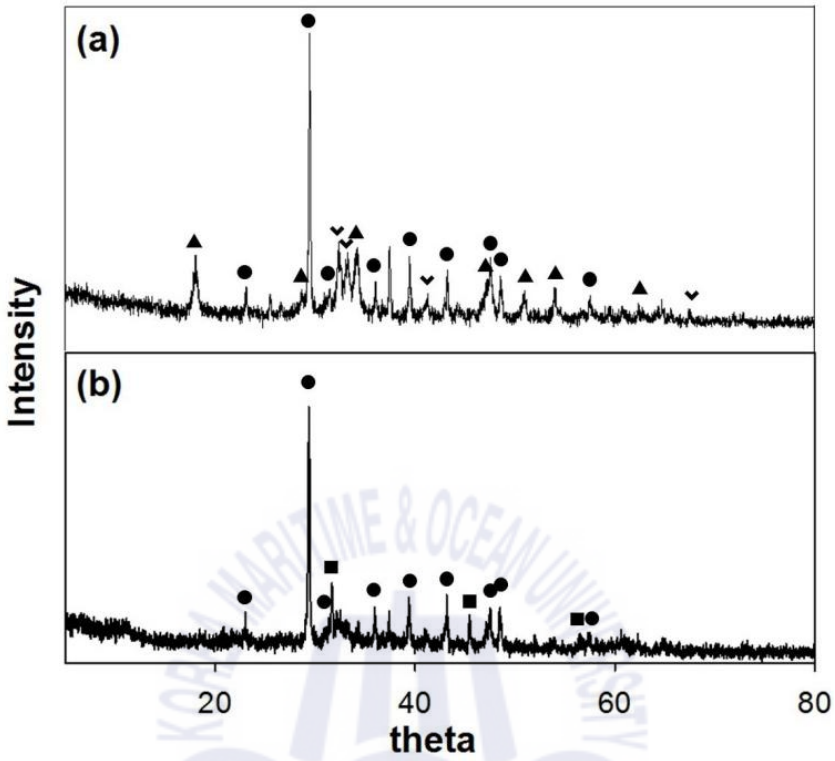

●: $CaCO_3$, ▲: $Ca(OH)_2$, ❯: CaO, ■: NaCl

Fig. 5. X-ray diffraction results: (a) raw paper sludge ash (PSA) and (b) solid obtained after filtering the mixture of PSA and brine when the ratio was 1:40.

The species that most influenced the pH in the suspension where the PSA and brine coexisted was the $Ca(OH)_2$ of the PSA. When a relatively small amount of PSA was added to the brine, the PSA to brine ratio was lower than 1:40, and most of the OH^- dissolved from $Ca(OH)_2$ was used to react with the Mg ion; thus, the pH remained lower than 10.8 (Fig. 4). In addition, this reaction boosted the formation of $Mg(OH)_2$ and dissolution of Ca from the PSA. On the other hand, if more PSA than required was added to precipitate the Mg of the brine, then the PSA to brine ratio was higher than 1:40, and the extra OH^- rapidly increased the pH to higher than 10.8.

Meanwhile, the B concentration was almost 0 mg/L when the ratio of PSA to brine was 1:40, which implied that most of the B in the brine precipitated as a solid phase (Fig. 4). Therefore, B was eluted along with the Mg as H_2SO_4 was added to the mixture of PSA and $Mg(OH)_2$ during the subsequent dissolution step.

1.3.3. Dissolution of $Mg(OH)_2$ using sulfuric acid

In many previous studies, acid solvents, such as HCl or acetic acid, were used to dissolve Mg from the solid phase (Dönmez et al., 2009; Teir et al., 2009; Özdemir et al., 2009). We used H_2SO_4 to dissolve the Mg from the mixture of $Mg(OH)_2$ and PSA. The reason for using H_2SO_4 was that the Mg of $Mg(OH)_2$ was eluted in the form of Mg^{2+} while the Ca of the PSA was converted into solid calcium sulfate ($CaSO_4$(s)), so a large amount of Ca would not be eluted into the solution (Lide, 2002). Mg was concentrated using H_2SO_4 with a volume that corresponded to one-fifth of the volume of the brine used in the previous step.

As shown in Fig. 6, as the concentration of H_2SO_4 increased, the concentration of Mg in the eluent at first increased proportionally, and then became constant. When the concentration of H_2SO_4 was higher than 1.0 M, the concentration of Mg in the eluent was approximately 8,500-10,000 mg/L, which was 3.5 to 4 times higher than that of the raw brine (2,340 mg/L). The efficiency of the Mg dissolution was approximately 72.6-85.5 %.

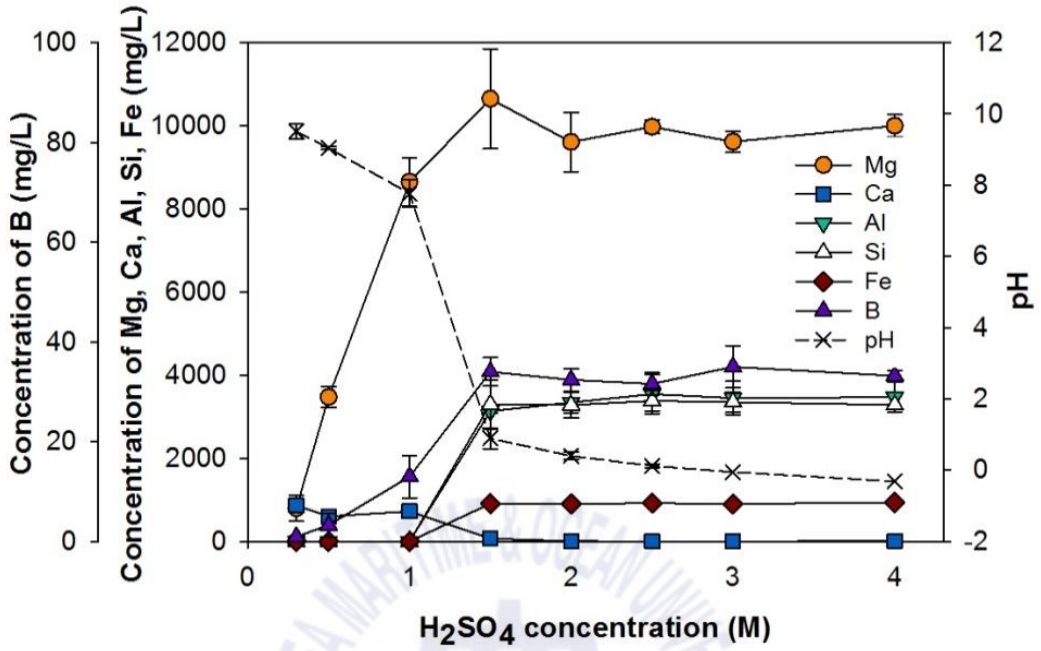

Fig. 6. Concentrations of Mg, Ca, Al, Si, Fe, and B and the pH of the eluent depending on the concentration of H2SO4.

The concentrations of Al, Si, and Fe showed similar trends, and they all originated from the PSA (Fig. 6). When the concentration of H_2SO_4 was lower than 1.0 M, the concentrations of Al, Si, and Fe were almost 0 mg/L, and when the concentration of H_2SO_4 increased to higher than 1.5 M, they suddenly increased.

Changes in the concentrations of Mg, Al, Si, and Fe were closely related to the change in pH of the eluent. At a relatively low concentration of H_2SO_4 (lower than 1.0 M), the pH of the eluent was as high as approximately 8-9, while the pH decreased rapidly to lower than 1 when the

concentration of H_2SO_4 was higher than 1.5 M. Therefore, when the concentration of H_2SO_4 was lower than 1.0 M, only Mg dissolved out from the mixture of $Mg(OH)_2$ and PSA (Smith et al., 2001; Pokrovsky & Schott, 2004). As the concentration of H_2SO_4 increased to higher than 1.5 M, the pH rapidly decreased and Al, Si, and Fe were eluted together.

Figure 7 shows the XRD results of the remaining solids after the eluent was prepared using H_2SO_4 with different concentrations of approximately 0.3-1.5 M. In the XRD results using 0.3 M H_2SO_4 and 0.5 M H_2SO_4, the peaks of $CaCO_3$ and $CaSO_4 \cdot 2H_2O$ coexisted, whereas only $CaSO_4$ peaks were observed when using 1.0 M H_2SO_4 and 1.5 M H_2SO_4. This indicated that when the concentration of H_2SO_4 was higher than 1.0 M, $CaCO_3$ was dissolved by excessive H_2SO_4 and $CaSO_4$ was produced.

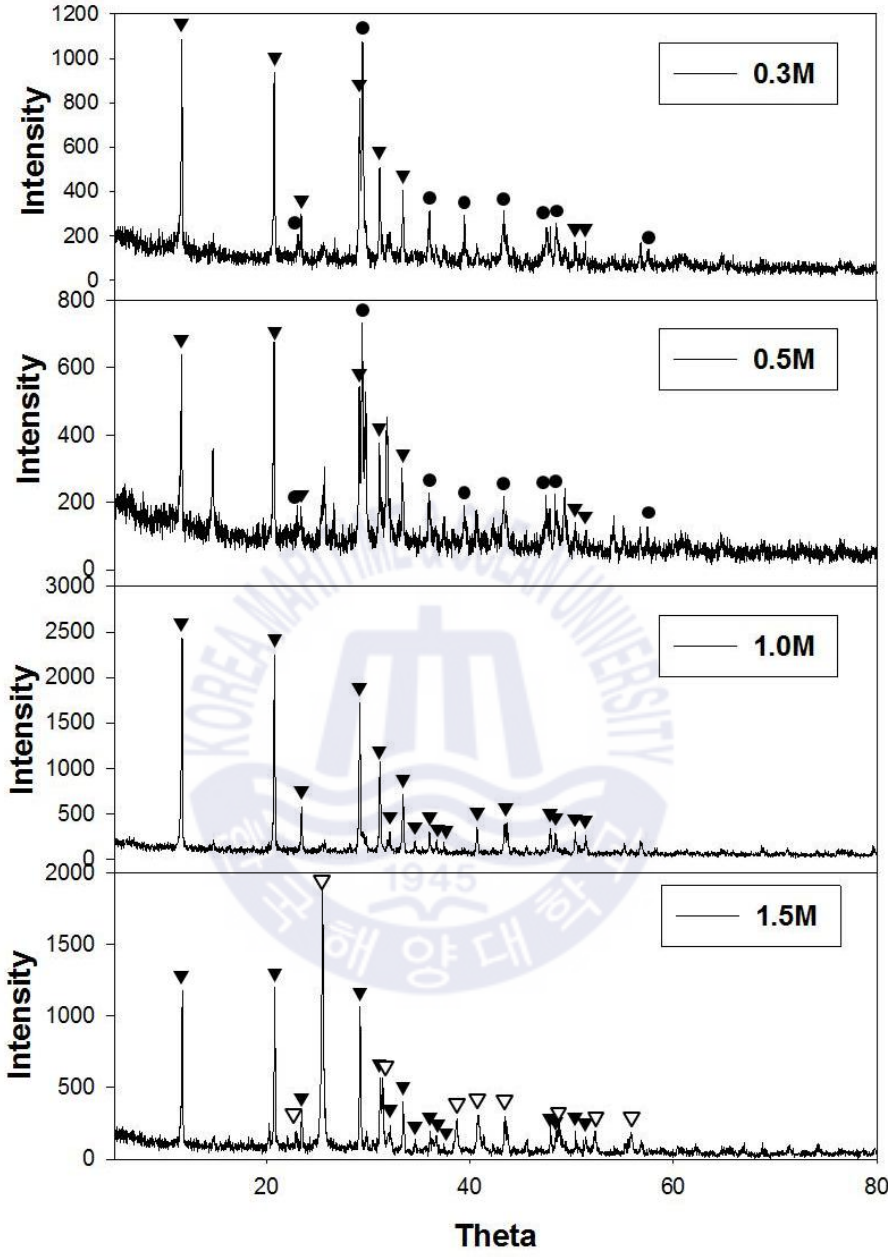

●: $CaCO_3$, ▼: $CaSO_4 \cdot 2H_2O$, ▽: $CaSO_4$

Fig. 7. X-ray diffraction results of solids remaining after dissolving Mg with 0.3-1.5 M H_2SO_4.

We found that at least 1.0 M H_2SO_4 should be used in order for the Mg concentration to be sufficiently high and to accelerate the precipitation reaction of $MgSO_4$ in the following step. The pH and the concentrations of components in each eluent obtained using 1.0 M H_2SO_4 are shown in Table 3. With 1.0 M H_2SO_4, a small amount of Ca and B were retained in the eluent with no other impurities, which was advantageous to obtain $MgSO_4$ with high purity. Therefore, we decided to use 1.0 M H_2SO_4 to produce the eluent for the next precipitation step.

Table 3. The pH and concentrations of the components of each eluent obtained using 1.0 M H_2SO_4

Concentration (mg/L)						pH
Mg	Ca	Al	Si	Fe	B	
8,600	725	0	0	0	13	7.5

1.3.4. Precipitation of $MgSO_4$ using ethanol

A certain amount of ethanol is injected into the eluent at once, we called it one-step process. On the other hand, if it injected in two portions, it is called two-step process.

1.3.4.1 One-step process

In this process, ethanol was added to the eluent to precipitate $MgSO_4$ as a solid. It was based on the characteristics of $MgSO_4$, which is rarely soluble in organic solvents (Lide, 2002). The amount of ethanol injected was expressed as the volume ratio of eluent to ethanol.

Figure 8 shows the change in Mg precipitation efficiency according to the volume ratio of eluent to ethanol. The Mg precipitation efficiency tended to increase as the amount of injected ethanol increased, in the form of an S-curve (Fig. 8). The precipitation reaction of $MgSO_4$ was closely related to the solubility of the $MgSO_4$ in the ethanol-water-$MgSO_4$ system. Zafarani-Moattar and Salabat measured the solubility of $MgSO_4$ in a mixed solution of water and ethanol at 25 °C (Zafarani-Moattar, 1997). As the portion of the ethanol increased in the mixture of water and ethanol, the solubility of the $MgSO_4$ decreased. Notably, the solubility of the $MgSO_4$ was almost 0 when the mass percentage of the ethanol was greater than 43.2, which corresponded to the volume ratio of water to ethanol of 1:1.03 when considering the ethanol density of 0.789. Thus, as shown in Fig. 8, the Mg precipitation efficiency reached its maximum when the volume ratio approached 1:1. We observed how the precipitation reaction occurred, and at

a volume ratio of approximately 1:0.6-1:0.8, the mixture of eluent and ethanol turned turbid with some suspended solids, which did not contain specific crystals, whereas at a volume ratio greater than 1:1.0, the solution rapidly crystallized and separated itself into the precipitate and supernatant. Therefore, in order to obtain $MgSO_4$ crystals and achieve high Mg precipitation efficiency, ethanol should be added to the eluent so that the volume ratio of eluent to ethanol is at least 1:1.0.

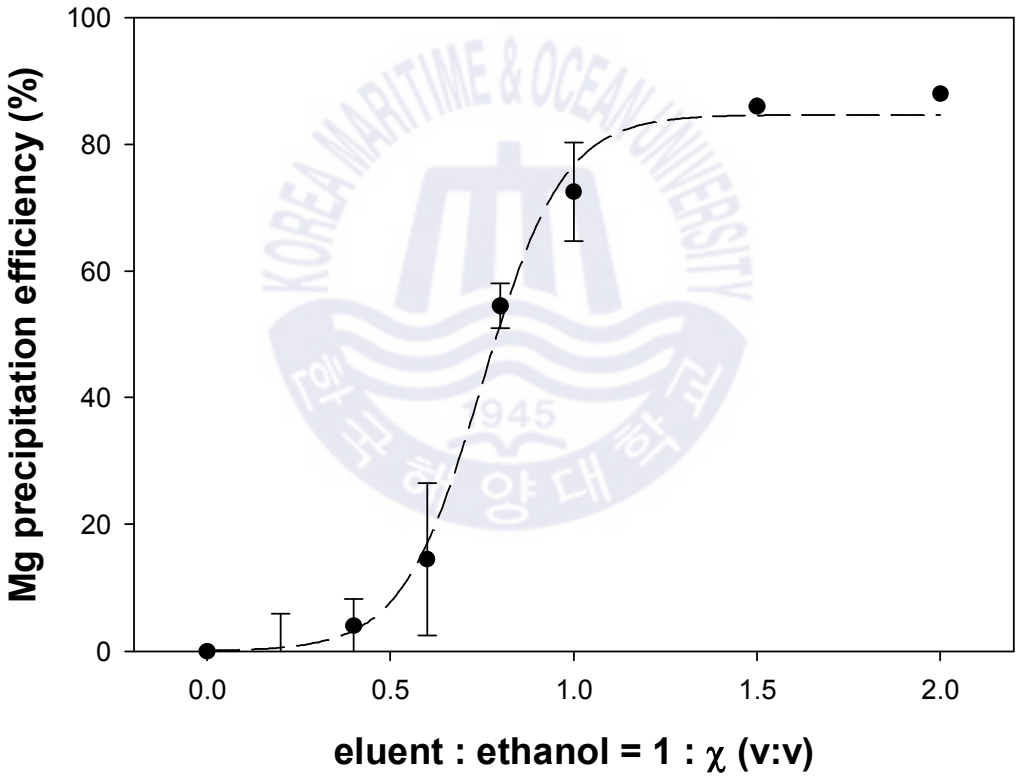

Fig. 8. Change in Mg precipitation efficiency according to the volume ratio of eluent to ethanol.

Figure 9 shows the amount of components remaining in the filtrate after $MgSO_4$ precipitation with a volume ratio of eluent to ethanol. The eluent contained a small amount of Ca and B as impurities (Table 3). As shown in Fig. 9, the amount of B in the filtrate did not change with the eluent:ethanol ratio, but the amount of Ca changed. The amount of Ca decreased when a small amount of ethanol (volume ratio of 1:0.4 or less) was injected into the eluent. Therefore, if ethanol was added in a ratio higher than 1:1, then the precipitated $MgSO_4$ would contain Ca as an impurity. Components such as Al and Fe were not present in the precipitated $MgSO_4$ because they were not present in the 1.0 M eluent (Table 3).

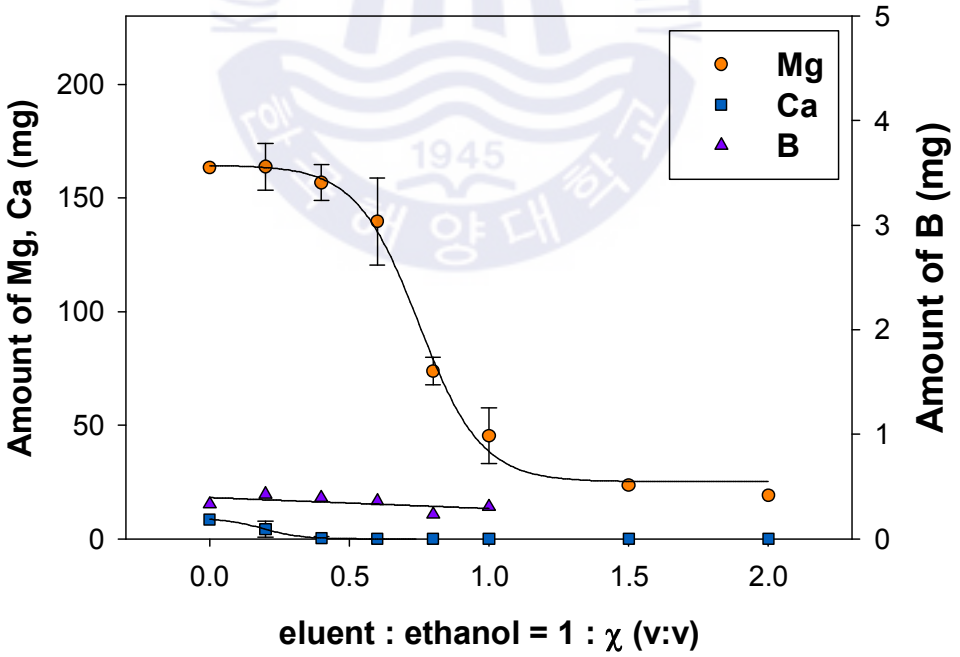

Fig. 9. The amount of components remaining in the filtrate after $MgSO_4$ precipitation depending on the volume ratio of eluent to ethanol

1.3.4.2 Two-step process

1.3.4.2.1 Eliminating Ca impurity from Mg eluent

Fig. 10 shows the XRD pattern of precipitated soild when the volume ratio of eluent to ethanol is 1:0.4. The main peaks of the solid were mateched with the $CaSO_4 \cdot 2H_2O$ which means the calcium in the eluent was precipitated and eliminated as the CaSO4 solid. Compare to the solubility of $MgSO_4$ in ethanol, $CaSO_4$ hardly dissolved in ethanol so Ca precipitation occurs first even small amount of ethanol injected. So by adding some amount of ethanol to Mg eluent and filtrating the mixture, the filtrated solution would be Ca-free Mg eluent.

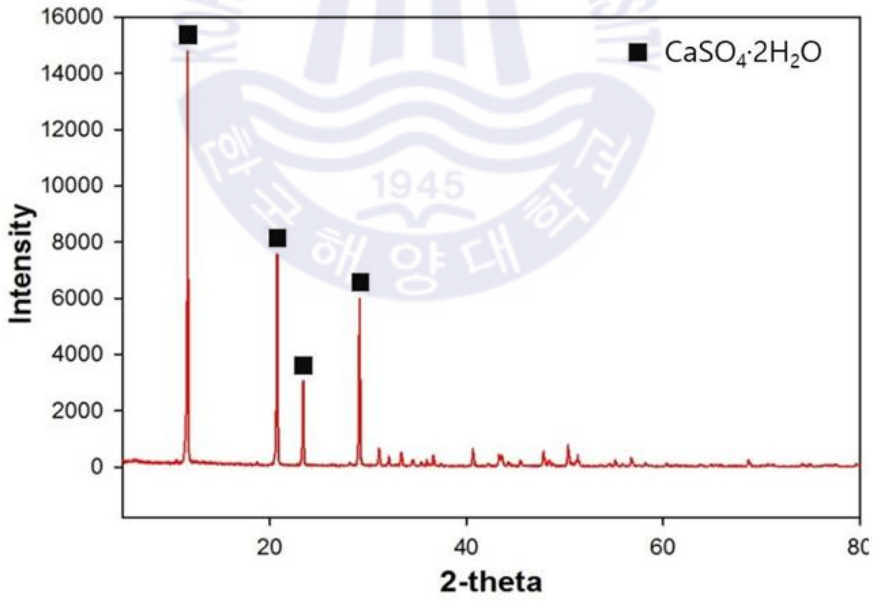

Fig. 10. XRD pattern of precipitated solid when the volume ratio of eluent to ethanol is 1:0.4

1.3.4.2.2 Precipitating Mg from Ca-free Mg eluent

As the volume of ethanol injected into the calcium-free magnesium eluate increased, the precipitation rate of magnesium increased. When the volume ratio was 1:1 based on the total ethanol injection amount, the magnesium precipitation rate was 90% or more. Furthermore, the efficiency of two-step process was higher than of one-step process.

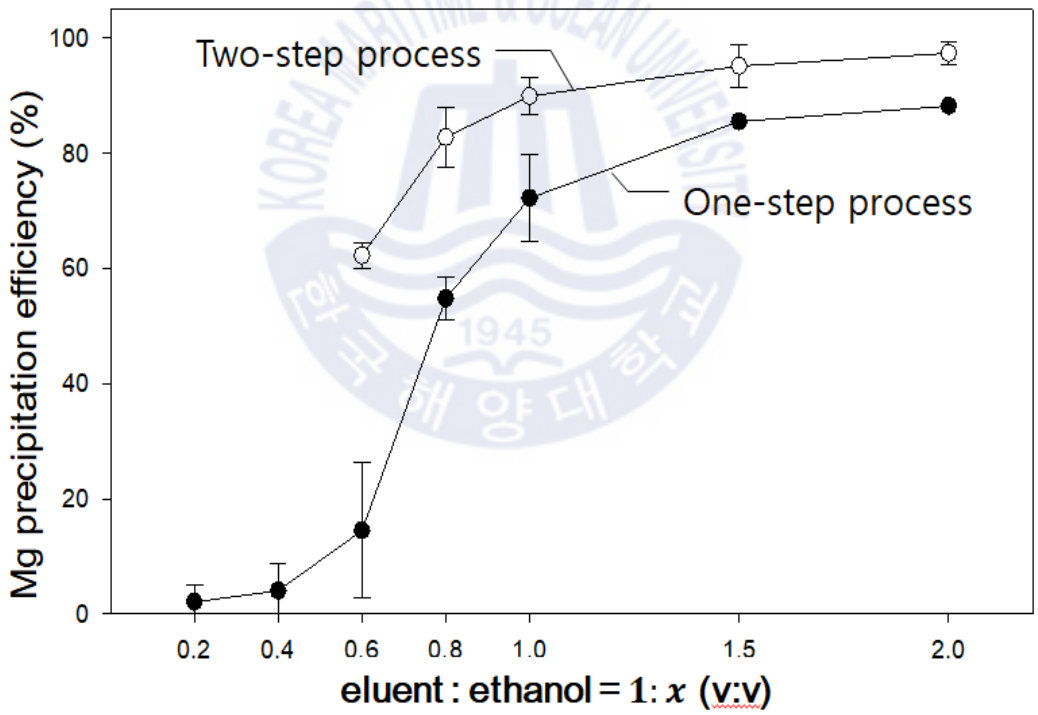

Fig. 11. Changes in precipitation efficiencies according to the volume ratio of magnesium eluent to ethanol

1.3.4.3 Comparing the phase purity depending on the ethanol adding method

We compared the purity of the $MgSO_4$ through one-step process and two-step process which is different in ethanol adding method. Table 4 is listed the component of $MgSO_4$ when the ratio of eluent to ethanol is 1:1 and the two different ethanol adding method were used. The purity of $MgSO_4$ for one-step process was 89.7 % with 6.72% of Ca impurity. On the other hand, for two-step process the purity of $MgSO_4$ was 99.8% without impurity.

Table 4 X-ray fluorescence results of MgSO4 precipitated using one-step process and two-step process

Ethanol adding method	S	Mg	Ca	Al	Fe	Si	Na	Cl	K
One-step process	68.6	21.1	6.72	-	-	-	3.01	0.63	-
Two-step process	74.1	25.7	-	-	-	-	0.13	-	-

As shown in Fig. 12, the peak of $MgSO_4 \cdot 7H_2O$ was mainly observed in the precipitated solid for two-step process(Fig. 12(b)). The $MgSO_4$ recovered for one-step process contained some $CaSO_4$ (Fig. 12(a)).

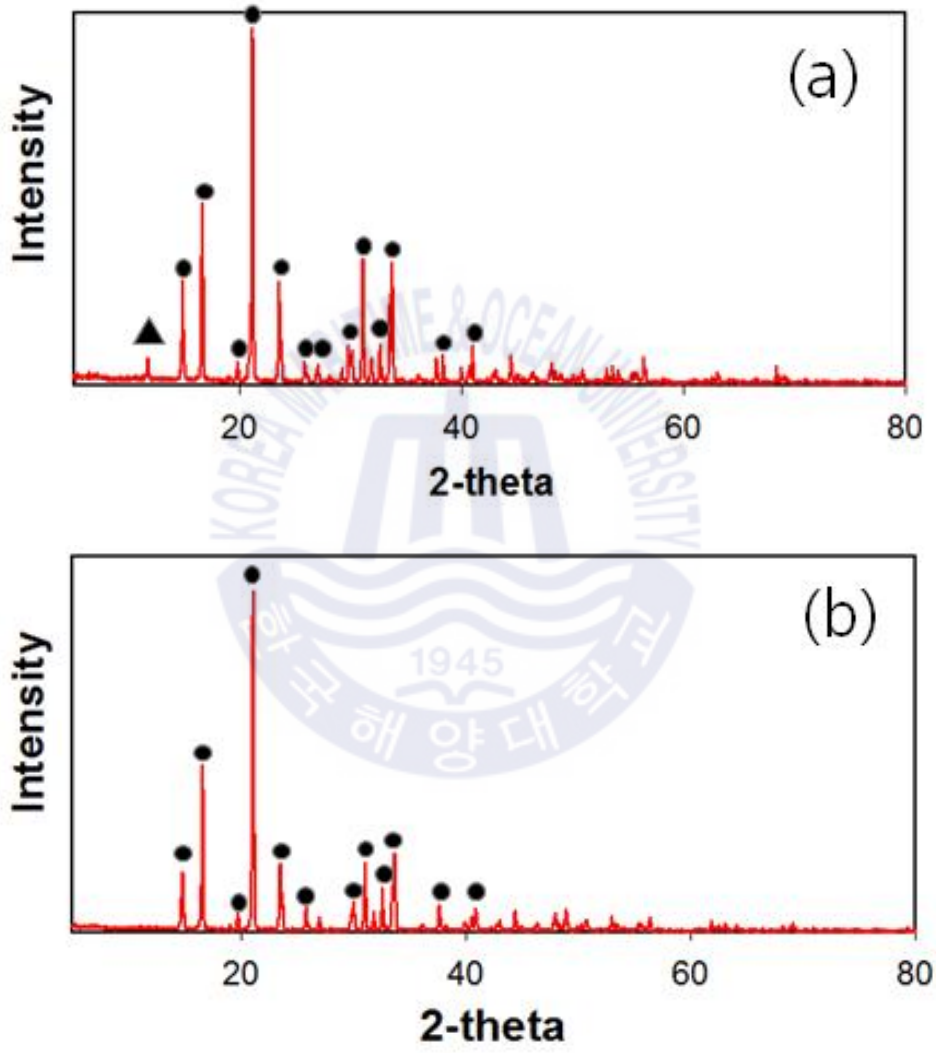

●: $MgSO_4 \cdot 7H_2O$ ▲: $CaSO_4 \cdot 2H_2O$

Fig. 12. X-ray diffraction results of the precipitated MgSO4 when the ratio of eluent to ethanol was 1:1 (a) One-step process and (b) Two-step process

1.4 Conclusion

In this study, we determined the optimum conditions of a three-step process to recover Mg from seawater desalination brine using an alkali industrial by-product, H_2SO_4, and ethanol. In the first step, involving the pre-precipitation of Mg, the op2.3.4.1 One-step process use of PSA facilitated the filtration of the $Mg(OH)_2$. During the dissolution of Mg, we produced an eluent with concentrated Mg by adding a mixture of PSA and $Mg(OH)_2$ to H_2SO_4 in a volume one-fifth of that of brine. We determined that the optimum concentration of H_2SO_4 was 1.0 M when the Mg dissolution efficiency was greater than 70 % and no impurities were eluted, except for Ca. By adding small amount of ethanol which is corresponding to 1:0.4 of Mg eluent to ethanol ratio, we eliminate te Ca impurity from Mg eluent. Finally, the precipitation of high-purity $MgSO_4$ led to the recovery of Mg in the form of $MgSO_4 \cdot 7H_2O$ by adding additional ethanol to Ca-free Mg eluent.

This technology is more economical than other existing technologies for recovering magnesium from seawater desalination brine for the two following representative reasons. First, the alkali industrial by-product was used instead of the existing expensive alkali precipitants. Second, ethanol and H_2SO_4 could be recovered and then reused in the process.

We assume that the seawater desalination brine and PSA used in this study for the three-step process could be replaced by seawater or bittern and

other alkali by-products. The optimal conditions could be derived in the same way as that proposed here, but the specific values of the optimal conditions may be different from the results of this study.

Chapter 2. Synthesis of magnesium carbonate from seawater

2.1. Introduction

Global warming is accelerating worldwide, and CCUS, a technology that captures, stores and uses CO_2, is being developed as a measure to reduce CO_2 emissions. Meanwhile, magnesium-based alloys are in the limelight as materials for weight reduction of automobile bodies and electronic devices. So that domestic demand for magnesium increases, while most domestic demand for magnesium comes from China or Japan. Therefore it is necessary to localize magnesium production technology in order to reduce the dependence on magnesium resources abroad. This study aims to develop a technology that can produce CO_2 while simultaneously producing magnesium from seawater, a quantitatively infinite resource.

2.2 Materials and Methods

2.2.1 Overall process overview: three-step process

The process of this technique is as follows (Fig. 13). First, Mg of seawater is precipitated in the form of $Mg(OH)_2$ using CaO (Mg precipitation step). $Mg(OH)_2$ is then added to a small amount of water, slurried, and then CO_2 is blown to remove calcium impurities and produce a solution with a higher Mg concentration than seawater (Mg concentration step). Finally, $MgCO_3$ is precipitated from the Mg concentrated solution ($MgCO_3$ production step).

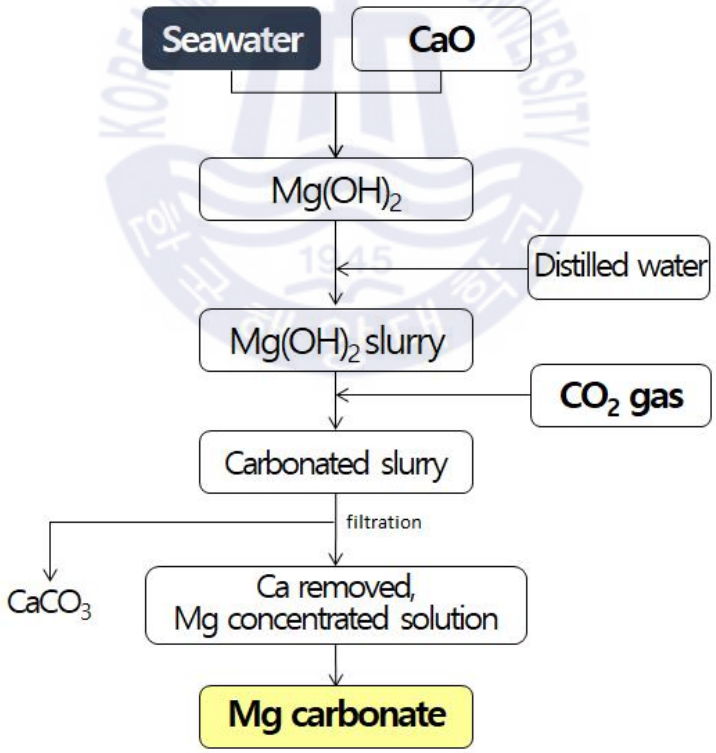

Fig. 13. Process for recovering Mg from seawater as $MgCO_3$

2.2.2 Pre-precipitation of Mg using CaO

By controlling the ratio of CaO to seawater, the amount of CaO required to precipitate all magnesium in seawater was determined. We injected the CaO to 100 mL of seawater with varying amount of 0.05-2 g, which is corresponding to the CaO to seawater ratio is 0.05-5% w/v, and stirred at 250 rpm for 1 hour. The mixture was filtered and the concentration of Mg and Ca in filtrate was measured by atomic adsorption spectrometer(AAS, Perkin Elmer, PinAAcle 500).

2.2.3 Carbonation of $Mg(OH)_2$

We prepared 0.6, 3.0, 6.0 L of seawater and CaO was added to each seawater so that the CaO injection amount was 0.5% w/v, followed by stirring at 250 rpm for 1 hour. After each mixture was centrifuged (8000 rpm for 20 minutes), the solids were recovered and the solids were each added in 300 mL of distilled water. The $Mg(OH)_2$ concentration of the slurry differs by approximately 0.1, 0.5 and 1.0 M, respectively. Carbonation reaction was carried out using 99.9% of CO_2 gas at different flow rates at 0.03, 0.3, and 3 L/min. CO_2 gas was injected into the slurry using a gas disperser and the slurry was stirred at a speed of 500 rpm using an impeller. During the carbonation reaction, the pH of the slurry was monitored using a pH meter, and small amount of the slurry was sampled and filtered. The concentration of Mg and Ca in filtrate was measured by AAS and the solids were dried and analyzed by X-ray spectrometer(XRD, Shimadzu, Optima 300).

2.2.4 Crystallization of $MgCO_3$

From the '2.2.3 Carbonation of $Mg(OH)_2$, only 5 Mg eluates which have the magnesium concentrated more than seawater has were used in this step. The Mg eluate was capped and left at room temperature for 5 days, and each sample was filtered under reduced pressure. The concentration of Mg and Ca in filtrate was measured by AAS and the solids were dried and analyzed by XRD.

2.3 Results and Discussion

2.3.1 Pre-precipitation of Mg using CaO

Figure 14 shows the concentration of Mg and Ca in the filtrate according to the CaO injection volume. Mg concentration decreased and Ca concentration increased as the amount of CaO injected. The concentration of Mg was 0 mg/L when CaO to seawater ratio was 0.5% w/v. It means that all the Mg of seawater can be precipitated under the above conditions. The reaction of CaO with Mg of seawater proceeds as follows.

$$MgCl_2 + CaO + H_2O \rightarrow Mg(OH)_2(s)\downarrow + CaCl_2$$

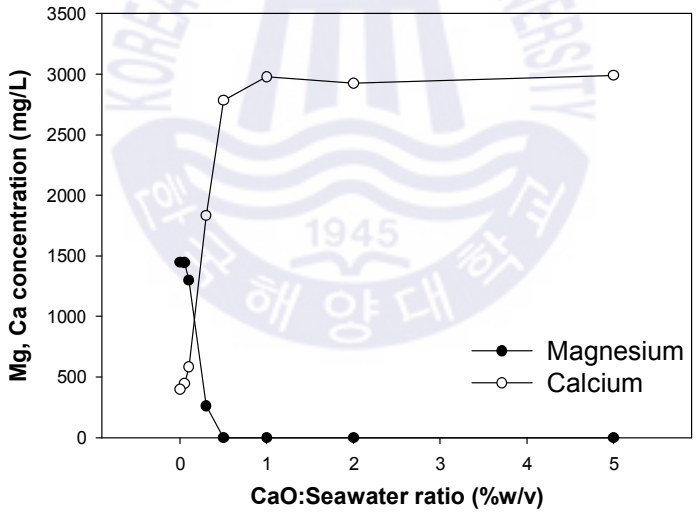

Fig. 14. Graph of Mg and Ca Concentration of Filtrate According to CaO Injection Volume

Figure 15 shows the XRD graph of solids precipitated at 0.5% of CaO to seawater ratio. Precipitated solids consisted mostly of $Mg(OH)_2$ and contained $CaCO_3$ and NaCl as impurities that is driven from seawater.

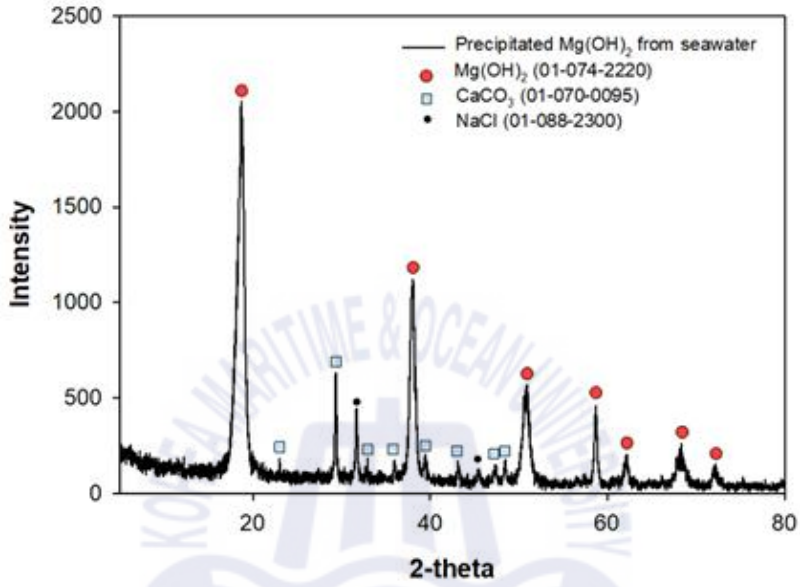

Fig. 15. XRD graph of precipitated solids when the CaO to seawater ratio is 0.5% w/v

2.3.2 Carbonation of $Mg(OH)_2$

In this step, the carbonation reaction was performed by injecting CO_2 into the $Mg(OH)_2$ slurry containing some of the Ca impurities obtained in the previous 'Mg precipitation step'. Here, the effects of $Mg(OH)_2$ concentration and CO_2 flow rate on the Mg leaching and Ca removal efficiency were investigated.

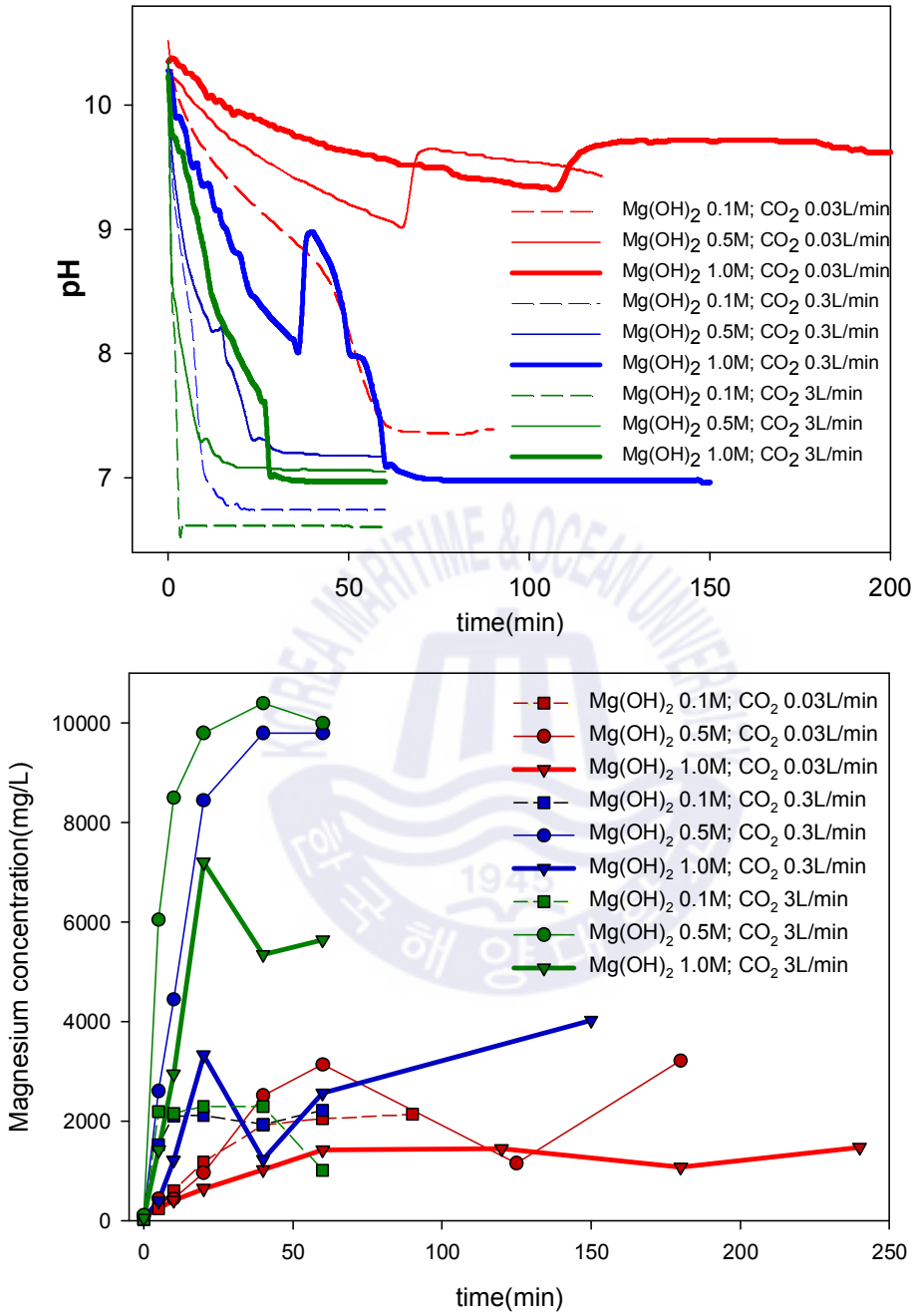

Fig. 16. Graph of pH and Mg concentration change according to carbonation reaction time according to $Mg(OH)_2$ concentration and CO_2 flow condition

As can be seen from the pH change graph, the rate of pH decrease was faster at high CO_2 flow rates regardless of the $Mg(OH)_2$ concentration. On the other hand, the graph of Mg concentration change shows that the CO_2 flow rate and $Mg(OH)_2$ concentration have a complex effect on the Mg concentration change during the carbonation reaction. Carbonation conditions with the highest Mg concentration are 0.5M $Mg(OH)_2$, CO_2 3L/min and $Mg(OH)_2$ 0.5M, CO_2 0.03L/min.

Mg elution efficiency was expressed as the percentage of Mg of the filtrate of the reactant after 60 minutes of carbonation relative to the Mg concentration of the initial carbonation slurry. Figure 4 is a graph showing the Mg elution efficiency for each condition using the above equation, and Figure 5. is an XRD graph of the residual solid after 60 minutes of carbonation time.

The conditions when the Mg elution efficiency is over 80% is correspond to the case where $Mg(OH)_2$ concentration is 0.1M, and the case where $Mg(OH)_2$ concentration is 0.5M and CO_2 flow rates are 0.3, 3L/min. The XRD analysis of residual solids under these conditions mostly showed a peak of $CaCO_3$. It can be seen that the reaction occurs that Mg(OH)2 is dissolved in the above conditions.

On the other hand, in the case of very low Mg dissolution efficiency is divided into two cases. First, in the case of d, g (when $Mg(OH)_2$ concentration is 0.5, 1.0 M and the CO_2 flow rate is 0.03L/min), a peak of $Mg(OH)_2$ was observed in the residual solid. This means that there was not

enough CO_2 supplied so that all the $Mg(OH)_2$ in the slurry could be dissolved. Secondly, for h and I (when $Mg(OH)_2$ is 1M and the CO2 flow rate is 0.3, 3L/min), a peak of $MgCO_3 \cdot 3H_2O$ was observed in the residual solid. This means that $Mg(OH)_2$ was dissolved during the carbonation reaction and then reacted with CO_3^{2-} to form carbonates.

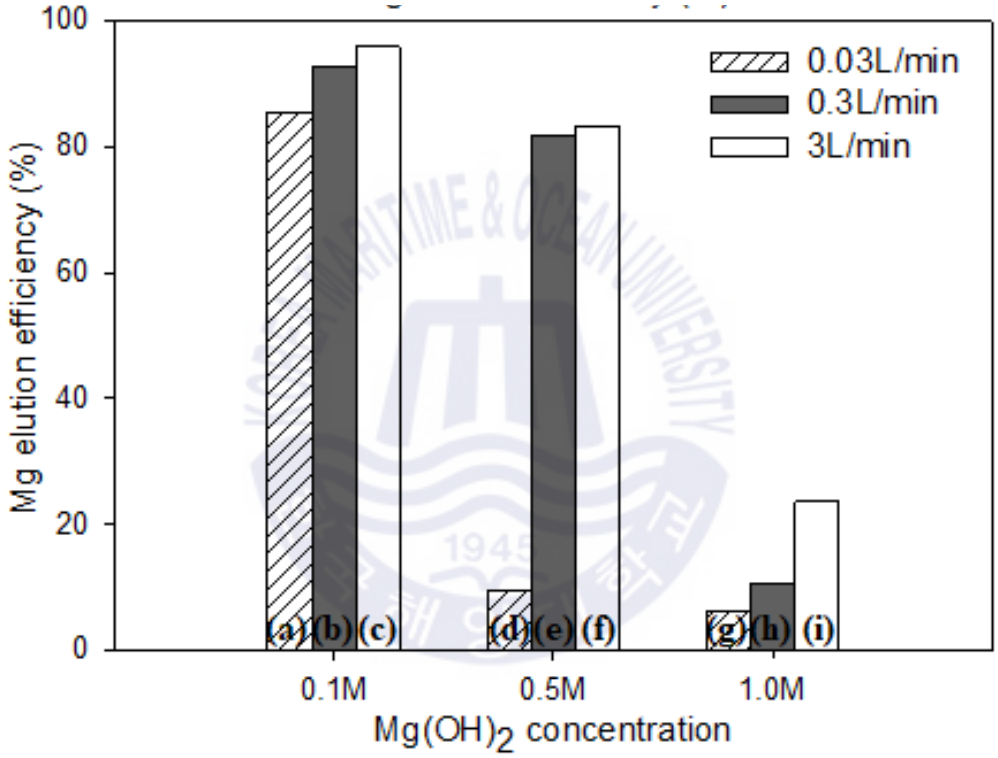

Fig. 17. Mg elution efficiency of after 60 minutes of carbonation depending on $Mg(OH)_2$ concentration and CO_2 flow rate

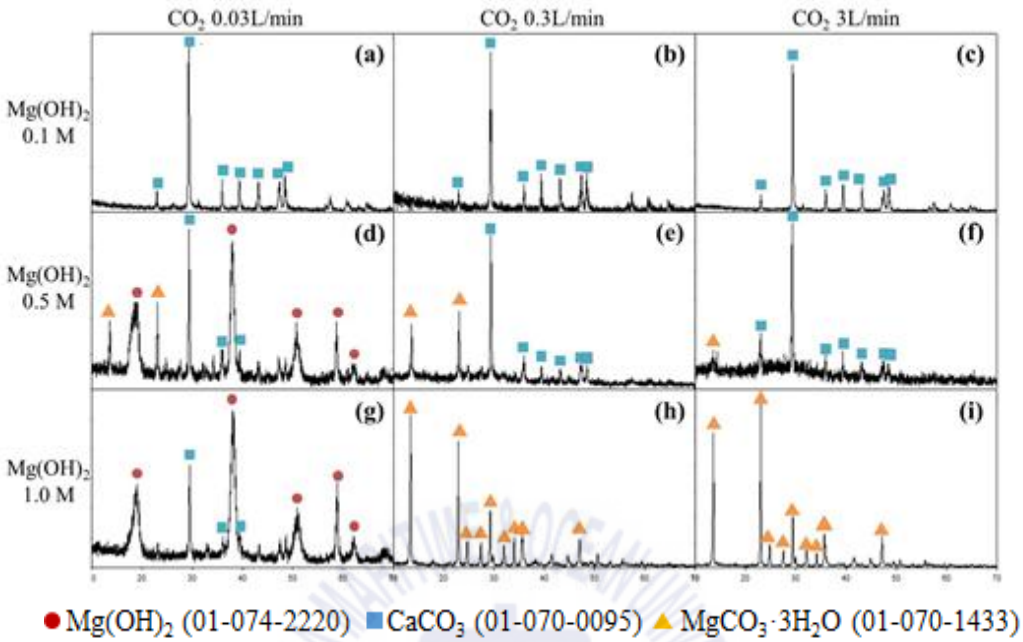

Fig 18. XRD graph of residual solids after 60 minutes of carbonation depending on $Mg(OH)_2$ concentration and CO_2 flow rate

2.3.3 Crystallization of $MgCO_3$

Table 1 lists the Mg and Ca concentrations of the five Mg eluates selected in the previous Mg elution step, and the respective eluates were allowed to stand at room temperature to precipitate solids and the filtrate was filtered.

Mg precipitation efficiency was high as 86.8 and 87.4% when the Mg concentration of Mg eluate was 9,800 and 10,000mg/L. XRD measurements of solids precipitated under these conditions showed that all peaks matched $MgCO_3 \cdot 3H_2O$ (Figure 19), yielding high purity $MgCO_3$.

Table 5. Mg precipitation efficiency depending on carbonation condition

Carbonation condition*	Mg eluate		Filtrates after $MgCO_3$ crystalized		Mg precipitation efficiency $\frac{A-B}{A} \times 100(\%)$
	Mg conc. (mg/L), A	Ca concentration (mg/L)	Mg conc. (mg/L), B	Ca concentration (mg/L)	
(a) 0.1,0.03	2,050	85.4	1,413	0	31.1
(b) 0.1,0.3	2,220	92.5	1,200	0	45.9
(c) 0.1,3	2,300	95.8	1,705	0	25.9
(e) 0.5,0.3	9,800	81.6	1,285	0	86.8
(f) 0.5,3	10,000	83.3	1,259	0	87.4

* $Mg(OH)_2$ concentration, CO_2 flow rate

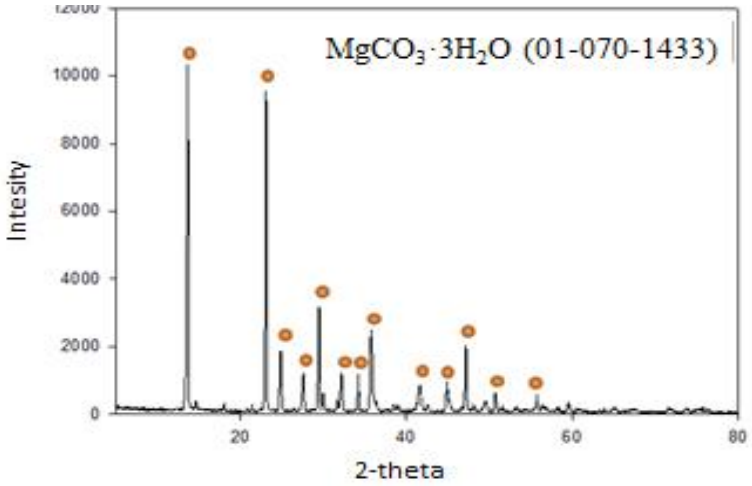

Fig. 19. XRD graph of synthesised $MgCO_3$ though three step of process

2.4 Conclusions

The three-step process for recovering Mg^{2+} in seawater in the form of high-purity $MgCO_3$ was presented, and the optimum conditions for each process to improve Mg recovery efficiency and synthesised MgCO3 purity were investigated. In the Mg precipitation step, Mg^{2+} of seawater was precipitated with $Mg(OH)_2$. In the Mg elution step, an eluate was prepared in which Mg concentration was higher than that of seawater mainly in forms of $Mg(HCO_3)_2$ and Ca impurities were removed as $CaCO_3$. High purity $MgCO_3$ was precipitated from the $Mg(HCO_3)_2$ eluate in the $MgCO_3$ precipitation step. The synthesised $MgCO_3$ was a high purity compound with no other impurities mixed.

Reference

Ahmad, N. & Baddour, R.E., 2014. A review of sources, effects, disposal methods, and regulations of brine into marine environments. Ocean & Coastal Management, 87, pp.1-7.

Barba, D. Brandani, V. Di Giacomo, G. Foscolo, P.U., 1980. Magnesium oxide production from concentrated brines. Desalination, 33, pp.241-250.

Casas, S. et al., 2014. Valorisation of Ca and Mg by-products from mining and seawater desalination brines for water treatment applications. Journal of Chemical Technology & Biotechnology, 89, pp.872-883.

Choi, Y. et al., 2018. Effect of chemical and physical factors on the crystallization of calcium sulfate in seawater reverse osmosis brine, Desalination, 426, pp.78-87.

Cipollina, A. et al., 2014. Reactive crystallisation process for magnesium recovery from concentrated brines. Desalination and water Treatment, 55, pp.2377-2388.

Cipollina, A., 2012. Integrated production of fresh water, sea salt and magnesium from sea water. Desalination and Water Treatment, 49, pp. 390-403.

Clontz, N.A., Johnson, R.T. McCabe, W.L. & R.W. Rousseau, 1972. Growth of magnesium sulfate heptahydrate crystals from solution. Industrial & Engineering Chemistry Fundamentals, 11, pp.368-373.

Dong, H. et al., 2018. Investigation of the properties of MgO recovered from reject brine obtained from desalination plants, Journal of Cleaner Production, 196, pp.100-108.

Dong, H., Unluer, C., Yang, E.H. & Al-Tabbaa, A., 2018. Recovery of reactive MgO from reject brine via the addition of NaOH. Desalination, 429, pp.88-95.

Dong, H., Unluer, C., Yang, E.H., & Al-Tabbaa, A., 2017. Synthesis of reactive MgO from reject brine via the addition of NH4OH, Hydrometallurgy, 169, pp.165-172.

Dönmez, B. Demir, F. & Laçin, O., 2009. Leaching kinetics of calcined magnesite in acetic acid solutions. Journal of Industrial and Engineering Chemistry, 15, pp.865-869.

Giwa, A. et al., 2017. Brine management methods: Recent innovations and current status. Desalination, 407, pp. 1-23.

Hoshino, T., 2015. Innovative lithium recovery technique from seawater by using world-first dialysis with a lithium ionic superconductor, Desalination, 359, pp.59-63.

Jeppesen, T., Shu, L., Keir G. & Jegatheesan V., 2009. Metal recovery from

reverse osmosis concentrate. Journal of Cleaner Production, 17, pp.703-707.
Lehmann, O., Nir, O., Kuflik, M., & Lahav, O., 2014. Recovery of high-purity magnesium solutions from RO brines by adsorption of Mg(OH)2(s) on Fe3O4 micro-particles and magnetic solids separation, Chemical Engineering Journal, 235, pp.37-45.
Lide, D.R., 2002. CRC Handbook of Chemistry and Physics, Taylor & Francis, 83rd Edition,
Melián-Martel, N., Sadhwani, J.J. & Báez, S.O.P., 2011. Saline waste disposal reuse for desalination plants for the chlor-alkali industry. Desalination, 281, pp.35-41.
Missimer, T.M. & Maliva R.G., 2018. Environmental issues in seawater reverse osmosis desalination: Intakes and outfalls. Desalination, 434, pp.198-215.
Mohammadesmaeili, F., Badr, M.K., Abbaszadegan, M. & Fox, P., 2010. Mineral recovery from inland reverse osmosis concentrate using isothermal evaporation. Water Research, 44, pp.6021-6030.
Özdemir, M., Çakır, D. & Kıpçak, İ., 2009. Magnesium recovery from magnesite tailings by acid leaching and production of magnesium chloride hexahydrate from leaching solution by evaporation. International Journal of Mineral Processing, 93, pp.209-212.
Park, M.J. et al., 2014. Recyclable composite nanofiber adsorbent for Li+ recovery from seawater desalination retentate, Chemical Engineering Journal, 254, pp.73-81.
Pérez-González, A. et al., 2014. Recovery of desalination brines: separation of calcium, magnesium and sulfate as a pre-treatment step, Desalination and Water Treatment, 56, pp.3617-3625.
Petersková, M., Valderrama, C., Gibert, O. & Cortina, J.L., 2012. Extraction of valuable metal ions (Cs, Rb, Li, U) from reverse osmosis concentrate using selective sorbents, Desalination, 286, pp.316-323.
Pokrovsky, O.S. & Schott, J., 2004. Experimental study of brucite dissolution and precipitation in aqueous solutions: surface speciation and chemical affinity control. Geochimia et Cosmochimica Acta, 68, pp.31-45.
R.H. Dave, P.K. Ghosh, 2005. Enrichment of Bromine in Sea-Bittern with Recovery of Other Marine Chemicals. Industrial & Engineering Chemistry Research, 44, pp.2903-2907.
Shahmansouri, A., Min, J., Jin, L. & Bellona, C., 2015. Feasibility of extracting valuable minerals from desalination concentrate: a comprehensive literature review. Journal of Cleaner Production, 100, pp.4-16.

Smith, A., Heckelman, P.E. & Budavari, S., 2001. The Merck Index: An Encyclopedia of Chemicals, Drugs, and Biologicals, Wiley.

Sorour, M.H., Hani, H.A., Shaalan, H.F., & Al-Bazedi, G.A., 2014. Schemes for salt recovery from seawater and RO brines using chemical precipitation. Desalination and Water Treatment, 55, pp.2398-2407.

Teir, S. et al., 2007. Dissolution of natural serpentinite in mineral and organic acids, International Journal of Mineral Processing, 83, pp.36-46.

Wan, A.-M., Mansoor, B. & Ahmad, F., 2016. Magnesium recovery from brines using exopolymeric substances of sulfate-reducing bacteria. Desalination and Water Treatment. 57, pp.25747-25756.

Zafarani-Moattar, M.T. & Salabat, A. 1997. Phase diagrams of aliphatic alcohols+magnesium sulfate+water, Journal of Chemical & Engineering Data, 42, pp.1241-1243.

Zahedi, M.M. & Ghasemi, S. M., 2018. Separation study of Mg^{+2} from seawater and RO brine through a facilitated bulk liquid membrane transport using 18-Crown-6, Journal of Water Reuse and Desalination, 7, pp.468-475.